

Rapid Mapping of Hydrological Systems in Tanzania Using a Towed Transient Electromagnetic System

by Denys Grombacher¹ , Pradip Kumar Maurya², Johan Christensen Lind², John Lane³, and Esben Auken⁴

Abstract

Limited knowledge of local groundwater systems often results in the failure of boreholes to yield water of the required quantity and quality. This is particularly problematic in the developing world, where financial resources are often limited, and failed wells represent a significant financial burden. To enhance understanding of local hydrological systems, noninvasive geophysical methods can aid the understanding of hydrogeological structures and identification of groundwater sources needed to optimize siting of wells. Here, we highlight the utility of a relatively new towed-transient electromagnetic system, called tTEM. This system is a rapidly deployable mobile geophysical method well-suited to cost-efficient characterization of local-to-regional groundwater systems. Results from tTEM surveys conducted in two refugee camps and several host communities in western Tanzania demonstrate the capability of the method to characterize shallow aquifer systems with high lateral and vertical resolution, with data collection typically exceeding 15 to 20 line-kilometers (km) per day. This work focuses on tTEM's ability to provide semiquantitative insights into regional hydrogeological settings when supporting data required for more rigorous interpretation/modeling is lacking. The system provided useful data within communities with low density of electrification and near buildings with metal roofs and walls. tTEM-derived resistivity profiles were correlated with limited local borehole lithologic information to develop conceptual models of the local groundwater systems. These models were used to successfully guide the siting of a production well and to identify future drilling targets in the refugee camps and surrounding communities.

Introduction

Safe drinking water is essential to human life, yet globally, roughly 800 million people lack access to basic drinking water services (World Health Organization [WHO]/United Nations Children's Fund 2008) from potable sources such as boreholes, piped water, or protected dug wells and springs. Many are forced to rely on untreated surface water sources at high-risk of contamination (WHO 2019), especially in areas where water sources are shared with animals and communities

practice open defecation. In addition, these high-risk water sources are often located at great distances from where people are living. Over 200 million people live in areas where the distance to the water source requires a minimum of 30 min per water collection trip (WHO 2019), a significant burden on daily life. In these situations, groundwater can be an attractive solution to meeting basic community water needs (Safe Drinking Water Foundation 2017), as groundwater is typically at lower risk of contamination (Klee 2013) than surface water, and may provide a sustainable safe-water solution in locations more convenient to the population.

In many circumstances, exploiting groundwater resources is hindered by the high cost of borehole drilling and the installation of related infrastructure (e.g., pumps, water pipes, water treatment equipment, storage tanks, and distribution points) which requires a significant financial investment by the governments, communities, or nongovernmental organizations (NGOs) that seek to develop groundwater for a safe water supply. Because a failed borehole represents a significant financial loss, it is imperative that boreholes are drilled in locations that maximize the likelihood of intercepting a safe sustainable water source. This can be a significant

¹Corresponding author: Hydrogeophysics Group, Geoscience Department, Aarhus University, Aarhus, Denmark; denys.grombacher@geo.au.dk

²Hydrogeophysics Group, Geoscience Department, Aarhus University, Aarhus, Denmark

³Hydrogeophysics Branch, United States Geological Survey, East Hartford, CT

⁴Geological Survey of Denmark and Greenland, Copenhagen, Denmark

Article impact statement: The value of a towed transient electromagnetic system for optimized well-siting is highlighted in a campaign in rural Tanzania.

Received April 2021, accepted August 2021.

© 2021, National Ground Water Association.

doi: 10.1111/gwat.13130

challenge in data-poor regions and/or complex geologic settings, where “data-poor” refers to situations where local hydrogeologic information is limited, nonexistent, or of poor quality.

Traditionally, borehole siting relies on some combination of local experience, geological mapping, preexisting topographical and geological maps, and/or analysis of airborne or satellite imagery. Surficial geologic expressions provide insight into subsurface geological structures and can help to identify the likely presence, spatial extent, and location of water-bearing units. The challenge is that these approaches suffer from great uncertainty about true subsurface conditions, particularly in complex geological settings. This uncertainty can culminate in poor drilling success rates—a common occurrence throughout much of the developing world (Wright 1992). For example, drilling projects in Ghana have reported success rates from 56% to 68% (Harvey 2004).

Near-surface geophysical methods augment traditional well siting techniques through noninvasive high-resolution imaging from the ground surface. Common methods include vertical electrical sounding (VES) for one-dimensional (1D) modeling, electrical resistivity tomography (ERT) for two-dimensional (2D) imaging (Beauvais et al. 1999; Coker 2012; Choudhury et al. 2017; Alle et al. 2018), magnetics (Sakala et al. 2014), seismic methods (Van Overmeeren 1981), nuclear magnetic resonance (Vouillamoz et al. 2014), and electromagnetics (Chongo et al. 2015; Magaia et al. 2018). These methods measure geophysical parameters that can be used to image and identify subsurface structures by exploiting contrasts in geophysical properties that can differentiate hydrological units—e.g., clays and sands corresponding to high- and low-electrically conductive materials (Palacky 1988).

In this work, we highlight the potential of towed-transient electromagnetic systems for cost-efficient local-to-regional hydrogeological mapping (Street et al. 2018; Auken et al. 2019). These systems are relatively easy and inexpensive to mobilize even in remote locations. The

towed system used in this work, called tTEM (Auken et al. 2019; Figure 1), consists of a compact-towed transmitter (Tx) frame (2 m wide by 4 m long) with a small receiver (Rx) coil trailing approximately 7 m behind the Tx. The system can be towed at speeds up to approximately 20 to 25 km/h over open terrain, obtaining between 800 and 2000 sounding measurements per second. The result is a suite of TEM soundings that can be used to produce 2D profiles or pseudo-three-dimensional (3D) images of complex hydrogeological systems.

In this work, we demonstrate the rapid mapping potential of the system at several refugee camps operated by the United Nations High Commissioner for Refugees and nearby host communities near Kigoma, in western Tanzania, in dire need of water to support the camp and community populations. The goals of the tTEM survey are threefold (1) to showcase the value of the system for the optimization of well-siting in regions with little hydrological information; (2) a demonstration of the ruggedness of the system and its suitability for challenging terrain; and, (3) the ability of the system to collect high-quality data within nonelectrified regions of communities where metal sheeting is a common building material. This work focuses on areas lacking significant supporting data and therefore discusses intentionally semiquantitative rapid field screening efforts that can aid in well-siting decisions. TEM systems can also be deployed with more quantitative objectives and/or directly coupled with hydrological models (Auken et al. 2017).

Background

Transient Electromagnetics

Transient electromagnetics (TEM) is a noninvasive geophysical measurement that involves pulsing strong currents in a Tx coil (Christiansen et al. 2006). These currents are turned off rapidly, where the turn-off generates a time-varying magnetic field in the subsurface



Figure 1. Picture of the tTEM system. The transmitter frame (red) is towed approximately 3.5 m behind the ATV, while the receiver coil (white box) is towed 7 m behind the transmitter. All instrumentation sits on the ATV, as well as a tablet streaming data and GPS location for data quality control and navigation.

that creates electrical currents (called eddy-currents) that propagate downward and outwards from the transmitter. The eddy-currents in turn produce a secondary time-varying magnetic field, the strength of which can be measured inductively at the surface using an open-air induction coil (called receiver coil). The observed voltages in the Rx coil can then be related to the strength and time-dependence of the eddy-currents at depth (e.g., Fitterman and Labson 2005). From the observed time-series of the decaying voltages in the Rx coils (often called the dB/dt curves) inversion methods are used to estimate the underlying electrical resistivity structures in the subsurface consistent with the observed data. Similar to VES, the standard output of a TEM sounding is a layered 1D model describing electrical resistivity with depth.

Knowledge of subsurface electrical resistivity distribution informs hydrogeological interpretation, as the imaging of structures of relatively consistent electrical properties can be used to delineate the thickness and spatial extent of underlying hydrogeologic units. The key underlying assumption is that distinct hydrogeological units can be differentiated by contrasts in their electrical properties. One common example is the ability to differentiate clay-rich materials from sands or gravels, where clay-rich materials tend to be very electrically conductive while sands and gravels are less electrically conductive.

Several types of TEM systems are commercially available, from static ground-based portable systems that utilize large (>40 m) Tx loops and stationary Rx coils to airborne systems that suspend TEM instruments beneath a helicopter or are flown with an airplane (Fountain 1998). Each of these systems has advantages and disadvantages. Ground-based systems are relatively affordable and easy to mobilize but cannot be efficiently deployed to provide dense coverage in heavily vegetated, forested, or rugged terrains. Airborne systems provide unparalleled spatial coverage but can be expensive to mobilize and often trade-off shallow, near-surface resolution for deep penetration. The tTEM was developed to fill the gap between these systems, providing a towable system that is inexpensive to mobilize, and is capable of rapidly mapping relatively large areas (e.g., >100 ha per day for gridded surveys, or as much as 50 line km per day of profile imaging). The tTEM system also provides high resolution at shallow depths, and has a typical depth of investigation ranging from 80 to 100 m.

Data Processing and Inversion

TEM data is most-commonly inverted using a 1D-forward operator, where a 1D layered earth resistivity model is used to explain the observed data at each sounding location. Although conceptually simple, the 1D-inversion approach enables successful imaging of complex 2D and 3D systems through high-density spatial coverage over long lines and/or large gridded areas. In this work, the TEM data processing workflow used Aarhus Workbench to implement laterally constrained-inversion

(LCI), which limits differences between neighboring resistivity models to produce spatially smooth images. The LCI approach addresses the ill-posedness of the inversion problem while also imposing the lateral structural continuity typical of many geological settings (Auken et al. 2005). Vertical smoothness constraints are also imposed, which result in model smoothness along the vertical direction. The smoothing constraint strengths can be varied during the inversion workflow to impose stronger or weaker continuity in both the horizontal and vertical directions. Alternatives to the LCI inversion workflow used here include 3D-inversion (Yang and Oldenburg 2012), Bayesian-frameworks (Minsley 2011), or different regularization schemes (Viezzoli et al. 2008; Vignoli et al. 2015).

In this work, the TEM model depth of investigation (DOI) is calculated using the approach outlined in Christiansen and Auken (2012). Because depths below the DOI lack the data support to be reliably interpreted, the DOI is used to determine and delineate “cutoff” depths along the imaged profile.

Geological Setting

The geological setting in northwestern Tanzania where the tTEM campaigns were conducted is a weathered regolith environment, believed to be of mafic or ultramafic origin based on the widespread observation of iron-rich laterite at the surface. This setting occurs given tectonic stability over geologic timescales, where erosion rates are exceeded by weathering rates, moderate relief to ensure drainage for efficient leaching, and a humid tropical environment (Butt et al. 2000). Figure 2 illustrates a cartoon of this regolith setting, based on a brief summary of the layers discussed in Butt and

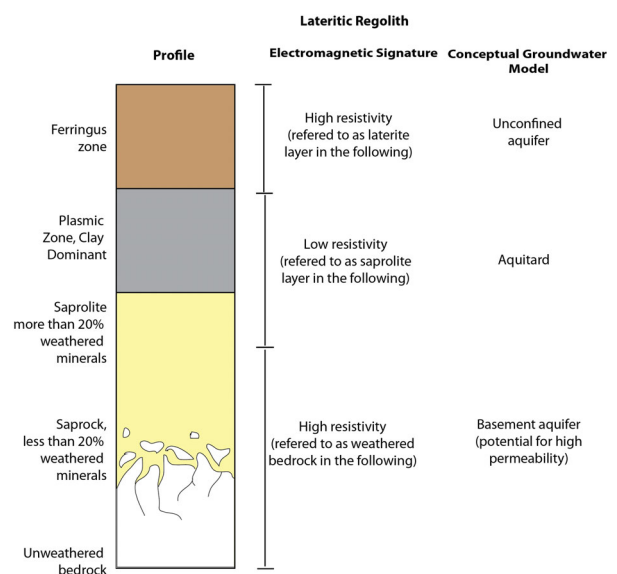


Figure 2. Schematic of the regolith setting in the surveyed areas. The electromagnetic signature and conceptual groundwater model columns illustrate the likely electrical signatures of the different regolith layers, and the underlying conceptual hydrogeological model used in the following interpretation of the resistivity profiles.

Zeegers (1992) and Butt et al. (1991). The regolith sits atop unweathered bedrock. At the base of the profile is the saprock, which has less than 20% weathered materials, and is home to an active weathering front where fresh bedrock is undergoing chemical weathering. Above the saprock, sits the saprolite zone containing more than 20% weathered materials. The boundary between these units is controlled by mineral mobility during weathering. This is not a sharp boundary, but rather a gradual decrease in weathering with depth. The plasmic zone, defined by a total loss of any fabric belonging to the host rock, sits atop the saprolite, is dominated by various clay-types. At the top is the ferruginous zone, rich in the most stable elements. In the surveyed regions in western Tanzania, the ferruginous zone was rich in iron-oxides, as evidenced by the red laterite soils and outcrops at the surface.

From an electromagnetic perspective, it is challenging to resolve each of these individual layers. Instead, the tTEM system will resolve a simplified version defined by contrasts in electrical properties—likely dominated by changing clay-contents. The center column of Figure 2 illustrates the anticipated tTEM resolvable profile. This simplified model is described by three-layers. The upper layer, termed the laterite layer in the following, is assumed to be an electrically resistive unit. This interpretation is based upon the observation of widespread shallow resistors in the surveyed areas where laterite was visible at the surface. This relationship is also supported by a borehole report at the Nyarugusu site, where a resistive layer in tTEM profiles was observed at the same depths as laterite in the borehole report (this borehole is discussed further in Results section). Electrical resistivity surveys conducted in nearby Burundi (less than ~50 km from several of the sites in the tTEM campaign) in a similar regolith setting report resistivity values for laterites exceeding 500 Ωm (Peric 1981). Underneath this layer is an increase in clay-content, corresponding to a layer termed saprolite in the following. For the saprolite layer, Peric (1981) reports resistivity values ranging from 5 to 25 Ωm , suggesting this layer can be differentiated from the overlying laterite by a transition to lower resistivity. The low resistivity of this unit is a consequence of its elevated clay-content. Elevated clay-contents are supported by the Nyarugusu borehole log, where low resistivity values are observed at depths described as clay-rich. Further support that the clay-rich saprolite has a low resistivity signature is the observation of marshy conditions, standing water and/or springs in areas where the low resistivity units in the tTEM images approach the surface. Beneath the saprolite is a gradual transition containing less weathering until the bedrock is reached. This gradual transition is termed the weathered bedrock layer in the following and is anticipated to correspond to a transition to higher resistivity values given its reduced clay-content. This assumption is based on the observation of higher resistivity values underneath the clay-rich layer at Nyarugusu, as well as the widespread observation of a transition to higher resistivity at depth in the tTEM

surveys. The following tTEM interpretations are based on these underlying resistivity-to-lithology assumptions.

In terms of groundwater systems, two aquifer systems are present in the region. The first is an unconfined aquifer that sits atop the clay-rich saprolite. Water is extracted from this aquifer using shallow hand-dug wells, or shallow-wells fitted with hand pumps or small motorized pumps in many of the communities. A second aquifer system is the basement aquifer that lies in the weathered bedrock at depth, where large volumes of water (>100 m³/h at a Nyarugusu borehole) are produced from greater depths. TEM is used to map regional extents of electrical structures in the subsurface, the geological interpretation of these units is based on the intersection of TEM results with available borehole information. Or in the case of no borehole information, it is assumed that the electrical unit to geological unit transform is the same as the nearest available borehole information. As such, subsequent interpretations and borehole siting recommendations that target the basement aquifer are based on an implicit assumption that the resistive unit at depth hosts a regionally expansive basement aquifer.

Limited additional information was available from the preexisting wells within the surveyed communities. The wells were generally drilled to depths ranging from 70 to 100 m for larger production (>20 m³/h) boreholes fitted with motorized pumps. These boreholes are steel-cased and screened near their bottom at depths where a basement aquifer composed of weathered bedrock is encountered. Several of these wells, where static water levels were available, displayed water levels at depths above the clay-rich saprolite layer—indicating the presence of a confined aquifer with head levels extending above the upper confining aquitard. A number of shallower steel-based wells (<30 m) fitted with hand-pumps also exist in the communities.

Results

Nduta Refugee Camp, Tanzania

In October 2019, tTEM surveys were conducted in the Nduta refugee camp and several nearby host communities. At the time, the Nduta camp was home to approximately 74,000 Burundian refugees. Water for the camp is sourced from two boreholes located near the western edge of the camp and from surface water extracted from a nearby river. River water quality is generally poor, with high turbidity and fluctuating levels of bacterial contamination. Eliminating the use of the surface water source required the development of additional groundwater resources. At Nduta, only two of four drilled wells were successful and in production. Information about existing boreholes (beyond well location, total depth and static water levels) or the local hydrogeology was limited to a general understanding of the regional information outlined in the geological background section.

Figure 3A shows a satellite image of the camp. The black lines in the figure delineate tTEM profile locations

determined suitable for processing and inversion. Portions of data collected in the interior of the camp were culled to eliminate soundings exhibiting the effects of (1) the presence of highly resistive subsurface materials that failed to produce observable signal levels (i.e., only instrumental noise is measured); and (2) induced-polarization, a phenomenon that generates data difficult to fit using a conventional electromagnetic model independent of frequency. These regions did not display exposed bedrock, but are likely areas with much thicker laterite cover or very thin saprolite layers; the geophysical data can only qualitatively constrain these regions to be resistive. Fitting tTEM sounding data impacted by induced polarization phenomena is the subject of ongoing research. For locations in the camp where data were culled because of low signal levels, the underlying subsurface can be qualitatively interpreted as very resistive to the depth of investigation. Given tTEM's inability to produce images of the subsurface in these regions (beyond qualitative classification as resistive) alternative regions are prioritized for well-siting recommendations, as the resistivity images cannot provide significant additional insights in this area.

In Figure 3B, a 3D-visualization of the tTEM resistivity profiles at the Nduta camp with a vertical exaggeration factor of 5 is shown. Much of the southern portion of the camp (bottom-most region) is underlain by a two-layer system, where an upper high-resistivity layer overlies a layer of lower-resistivity. These layers are interpreted as layers of laterite and saprolite, respectively. The tTEM system is unable to penetrate beneath the low-resistivity layer underlying the southern portion of the camp, typically producing models with a DOI ranging from 50 to 75 m. The location of the two existing producing wells at the camp are highlighted by the red circles in Figure 3A. The producing wells were drilled to depths of 70 and 65 m, respectively; depths beneath the depth of investigation for the nearest tTEM.

Figure 4 illustrates a resistivity profile representative of the Nduta region. The profile location corresponds to the blue line in the satellite image in Figure 3A. The image shows a vertical slice into the subsurface, where the vertical axis corresponds to elevation and the horizontal axis to the distance along the profile. The profile runs from its northernmost point (left) to its southernmost point (right). This image illustrates the lateral continuity of the two-layer structure, which extends from the location of the existing wells (left-side of Figure 4) to the southernmost region of the camp into the area near the convergence of two streams. The area where the streams intersect also coincides with the lowest elevations in the region surrounding camp. Using this information, a borehole near the right-hand side of the upper profile in Figure 4, was recommended, as it represents a location with a similar subsurface structure as that at the existing productive wells as well as at a lower elevation within a larger catchment area. At the time of writing, this site has not yet been drilled.

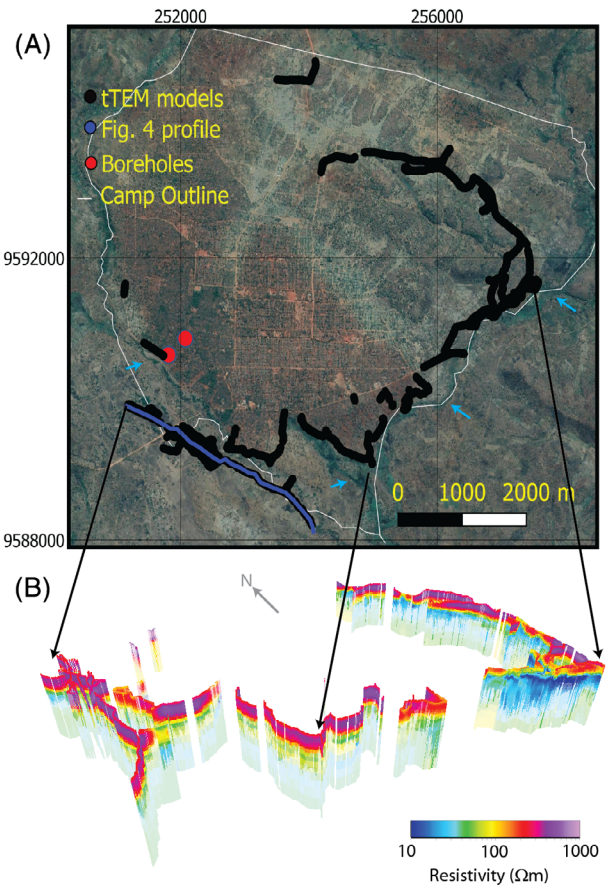


Figure 3. (A) Satellite image of Nduta refugee camp, western Tanzania (referenced to WGS 84 UTM Zone 36S). Map data: Google, CNES/Airbus. (B) Visualization of the resistivity models collected in the vicinity of Nduta. Arrows indicate the corresponding locations in (A) and (B). Note that (B) contains a vertical exaggeration factor of 5. The height of each vertical bar is approximately 100 m. Blue arrows in (A) mark the locations of nearby streams.

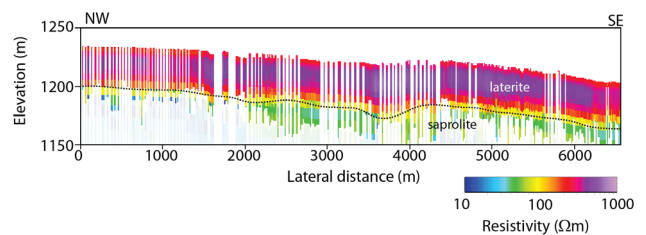


Figure 4. A resistivity profile at the Nduta camp that correspond to the location of the blue line in Figure 3A. The upper laterite unit displays relatively consistent thickness and is continuous across the profile. The laterite layer is underlain by a continuous saprolite.

Nyarugusu Refugee Camp, Tanzania

The tTEM survey conducted in Nyarugusu refugee camp provided approximately 70 km of data over a 4-day acquisition period. In Figure 5A, a satellite image of the camp is shown, with black lines delineating tTEM survey locations determined suitable for processing and inversion. The tTEM surveys were focused on the

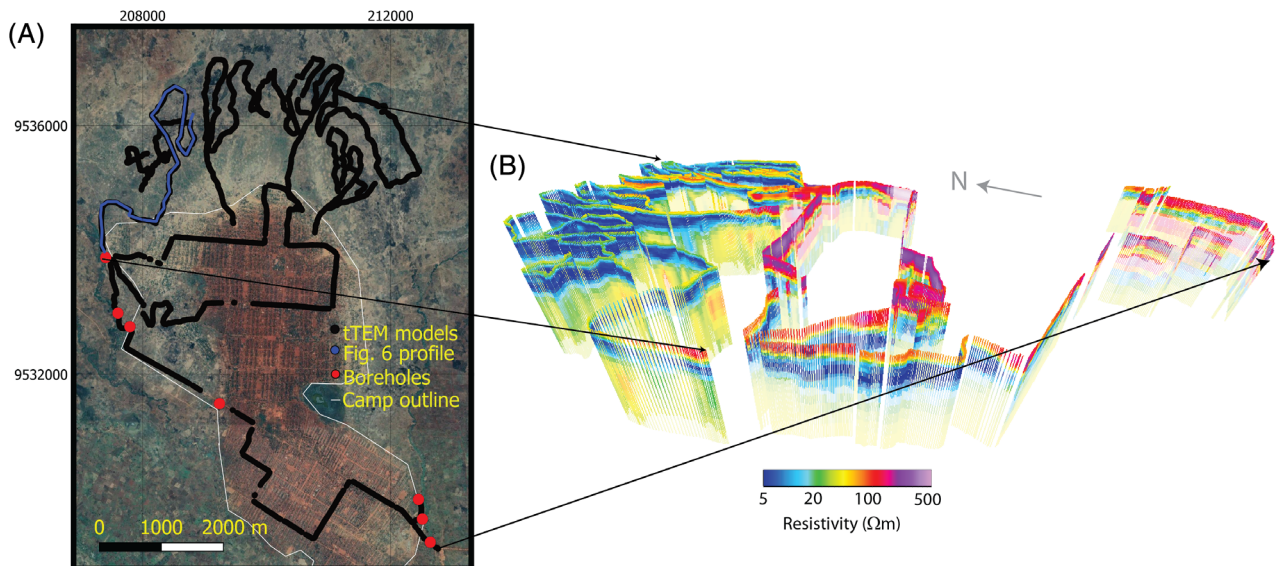


Figure 5. (A) Satellite image of Nyarugusu camp (referenced to WGS 84 UTM Zone 36S). Map data: Google, Maxar Technologies, CNES/Airbus. (B) Visualization of the resistivity models collected in the vicinity of Nyarugusu. The arrows indicate the corresponding locations in (A) and (B). Note that (B) contains a vertical exaggeration factor of 5. The height of each vertical bar is approximately 100 m.

northern region of the camp, which was prioritized as a likely future expansion area. At the time of the survey, the Nyarugusu camp was home to approximately 170,000 Burundian and Congolese refugees, with camp water supplied from surface water extraction, and augmented by several production wells. Concerns about surface water quality and the growing demands of downstream users motivated camp officials to explore development of an entirely groundwater-sourced water supply.

In Figure 5B, a 3D visualization of the tTEM resistivity profiles at the Nyarugusu camp with a vertical exaggeration factor of 5 is shown. The orientation of the 3D visualization has the western region of the camp in the foreground, and the left and right directions correspond to north and south, respectively. At Nyarugusu, a laterally consistent layered structure is observed, with much of the region corresponding to an upper high-resistivity layer (interpreted as laterite), underlain by a low-resistivity layer that overlies a third higher resistivity layer at the model base. In the most north-eastern region (left-hand side of Figure 5A) the low-resistivity (blue layer) approaches the surface in an area observed to have ponded surface water, consistent with an interpretation of the low-resistivity layer as a clay-rich saprolite. The continuity of the three-layer structure, which extends from the location of the highly productive borehole in the northwestern region of the camp (highlighted by the location of a black arrow in Figure 5A) throughout the northern region of the camp is further illustrated by the resistivity profile shown in Figure 6. The three-layer structure is laterally consistent across the profile, with the resistive overburden thinning at the northern-most region (right side) of in Figure 6, again coinciding with an area of ponded surface water.

At Nyarugusu, seven boreholes have been drilled with four successfully used for production. The three

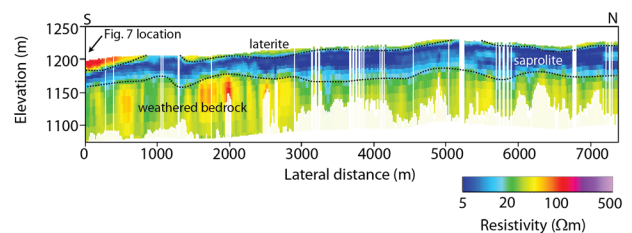


Figure 6. A resistivity profile from Nyarugusu camp corresponding to the blue line in Figure 5A. The three-layer system discussed in Figure 2 is present in this profile. The upper laterite is thin across much of the profile, with the underlying saprolite varying in thickness across the profile. A higher resistivity layer (weathered bedrock) is imaged at the base and is continuous across the profile.

boreholes near the southern entrance of the camp (bottom right corner of Figure 5A) are completed to depths of approximately 70 m and produce about 25 m³/h. A borehole drilled near the north-west corner of the camp was drilled to a depth of 98 m, with a screened interval from 68 to 94 m in a weathered bedrock interval. In Figure 7, a simplified lithologic log produced from drill cuttings at this borehole is shown. The cuttings generally describe a three-layer system, consistent with the resistivity images in Figures 5 and 6. The lithologic log shows a transition to a more clay-rich layer at depths of 15 to 20 m. At about 50 m, a transition zone consisting of large cobbles and a reduced abundance of clay was encountered. Minor water strikes occurred near 15 m (where the clay-abundance increases) and at 76 and 81 m, with major water strikes noted by the driller at 91, 93, and 95 m (blue arrows in the lithology log). Screens were installed over the 70 to 95 m interval. Field testing indicates the well produces approximately 100 m³/h. In Figure 7, a comparison between the

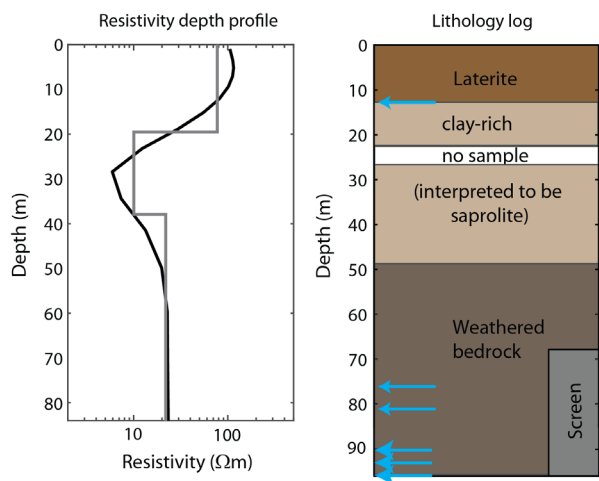


Figure 7. Comparison of the 1D-resistivity depth model produced by tTEM near a productive borehole at the Nyarugusu camp and a generalized lithologic log produced from drill cuttings. Black and gray profiles correspond to smooth- and three-layer inversion models of the same data set. Blue arrows in the lithology log indicate the depths of reported water strikes during drilling.

lithologic log and the resistivity model from the nearest tTEM sounding (about 50 m away, because borehole is surrounded by fencing) is shown. The resistivity models predict a transition to lower resistivity at the depth where abundant clay-fraction is observed in drill cuttings. At greater depths the transition to a higher resistivity zone beneath the low-resistivity layer correlates with a drop in clay-fraction in the drill cuttings, and the higher resistivity layer at the base appears to coincide with the transition to less-weathered bedrock. The borehole is screened

in the higher resistivity layer interpreted as weathered bedrock. The resistivity model is truncated at DOI of 85 m. The interpretation of the three dominant structures in the resistivity profile—where the upper resistive layer corresponds to a laterite layer, the low-resistivity layer is the clay-rich saprolite layer, and the higher resistivity at the base consists of weathered bedrock with a relatively low clay-content, is consistent with the lithology log.

The tTEM survey results illustrated in Figures 5 through 7 and the correlation of the models with the available borehole drilling information indicate that the productive zone intercepted by the northwestern borehole likely underlies much of the northern region of the camp. The lateral continuity of the local geology indicated by the tTEM survey results suggests that wells sited in the northern region are likely to encounter similar lithologic conditions as the northwestern borehole. At the time of writing, no additional wells at Nyarugusu have been drilled.

Makele, Tanzania

The community of Makele is located near the Nyarugusu camp, approximately 3 km from the southern camp entrance. Makele has a population of approximately 5000. In Figure 8A, a satellite view of the community is shown, with red dots identifying the location of shallow wells used by the community. No lithologic or well construction information was available for the community wells, other than anecdotal information provided by local officials indicating that the boreholes were drilled to a maximum depth of 30 m. Most wells are fitted with hand-pumps, with the exception of a few wells utilizing electric pumps in community interior. A hand dug well, marked by the orange circle, is present in the south-east corner of the community, where a water depth of approximately 2 m

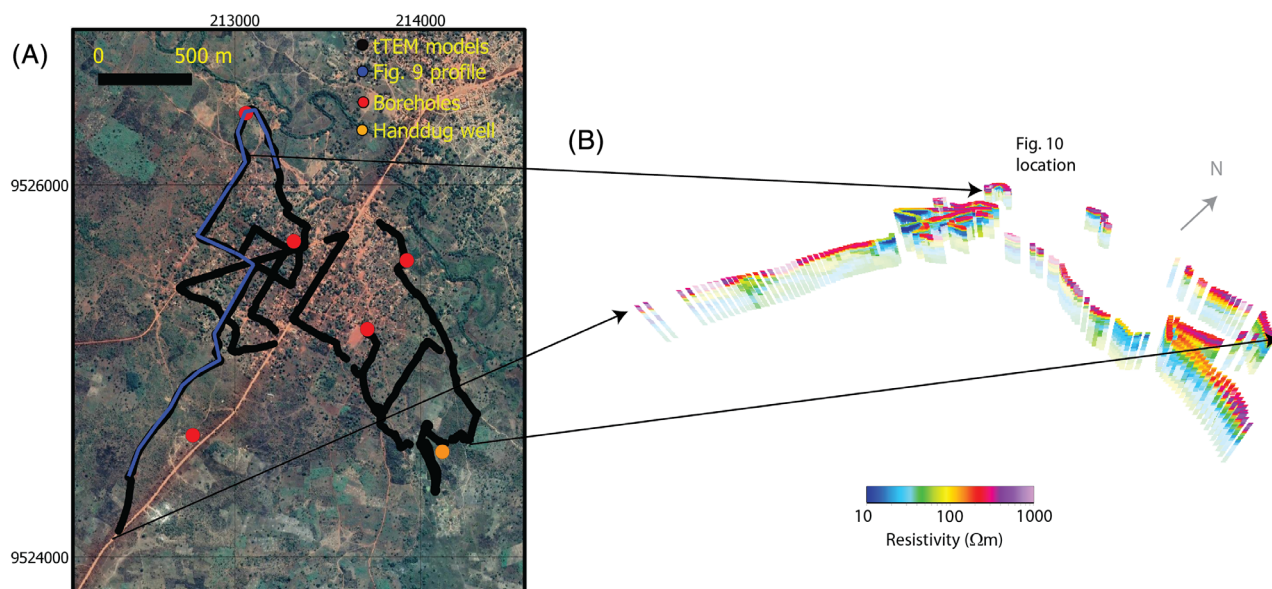


Figure 8. (A) Satellite image of Makere, western Tanzania (referenced to WGS 84 UTM Zone 36S). Map data: Google, CNES/Airbus. (B) Visualization of the resistivity models collected in the vicinity of Nyarugusu. The arrows indicate the corresponding locations in (A) and (B). Note that (B) has no vertical exaggeration in this case. The height of each vertical bar is approximately 100 m.

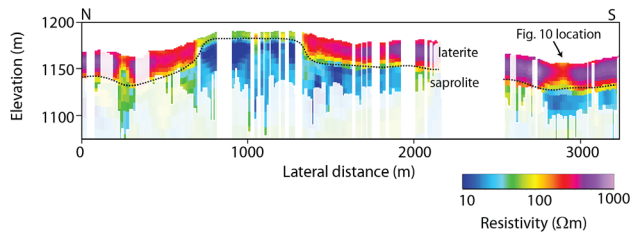


Figure 9. Resistivity profile corresponding to the blue line in Figure 8A. The upper laterite layer is present across much of the profile but thins at x -positions ranging from approximately 700 to 1300 m. The saprolite is continuous across the profile, with a transition towards higher resistivity at depth observed at several locations (e.g., ~2900 m).

below land surface was observed, indicating the presence a shallow unconfined surficial aquifer. The presence of a shallow surficial aquifer is further supported by the presence of two nearby natural fishponds (~100 m from the orange circle) and reports of seasonal flooding. Given the proximity of Makere to Nyarugusu, a similar lithologic setting was anticipated.

The tTEM survey conducted in Makere produced approximately 12 km of tTEM data over a 1-day acquisition period. In Figure 8, black lines delineate tTEM survey locations determined suitable for processing and inversion.

In Figure 8B, a 3D visualization of tTEM resistivity profiles acquired in areas surrounding Makere are shown. The resistivity structures define a three-layer system, similar to that observed at Nyarugusu, with an upper resistive layer underlain by a more conductive unit, with a transition to higher resistivities at greater depths. In Figure 9, a resistivity profile from Makere is shown, which transects the western portion of the community (terminating near the river, which corresponds to the location marked a black arrow in Figure 8). The location of the profile in Figure 9 is highlighted by the blue line in Figure 8A. In Makere, the three-layer structure is laterally continuous, with the depth and thickness of the intermediate low resistivity unit varying across the community. This variation is especially apparent between the positions spanning from 700 to 1300 m linear distance in Figure 9. Two hand dug seasonal wells, (~15 to 20 m deep) in the center of this interval were both dry at the time of the survey, suggesting that these wells intercept the intermediate low-resistivity (saprolite) unit which is not a producing unit during the dry season.

Based on the tTEM imaging results, a well was sited near the 2950 m position in Figure 9. This location was proposed due to the similarity with the three-layer structuring observed at the productive well site at Nyarugusu, and the low elevation adjacent to the river. In Figure 10, the resistivity depth model at this site is shown, with a smooth model (that displayed in Figure 9) and a three-layer inversion. Figure 10 also indicates the depths of major layer boundaries encountered during drilling—highlighted by black lines at the right of the profile. The layer boundaries were identified through

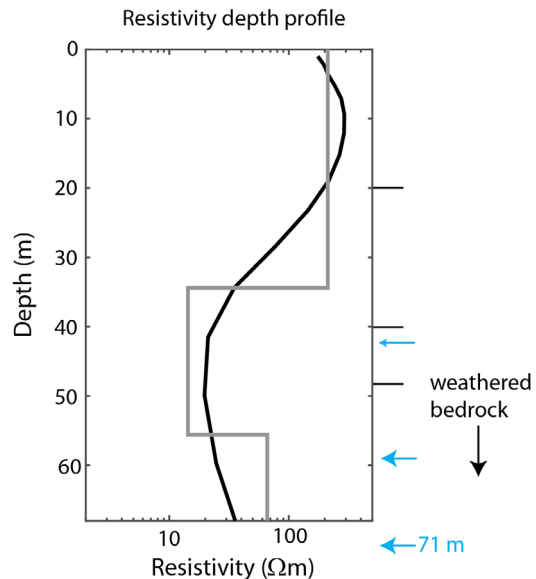


Figure 10. Resistivity depth profile at the location of the drilled borehole in Makere. Black and gray lines correspond to smooth and three-layer inversions respectively. Black lines on the right of the profile indicate the locations of layer boundaries identified by on-site engineer, while blue arrows indicate water strike depths.

visual inspection of drill cuttings on site. Detailed interpretation of the units encountered during drilling is not available beyond that the bottom layer corresponds to highly weathered bedrock. Water strikes were reported at depths of 43 m (minor), 59 m (major), and 71 m (major) and are marked by blue arrows in Figure 10. Field testing of the well indicates a potential yield exceeding 120 m³/h. The tTEM resistivity depth model is consistent with layer boundaries observed during drilling. The smooth inversion model begins a transition toward lower resistivity values beginning at the 20 m boundary, and also displays a transition toward higher resistivity values over a depth range consistent with the observed layer interface at 48 m, marking the transition into weathered bedrock.

tTEM Data Collection Within and Near Nonelectrified Communities

The presence of electrical infrastructure (e.g., powerlines) can inhibit the use of electromagnetic geophysical methods, such as tTEM. However, many communities in developing nations are not electrified, or are only partially electrified, including the refugee camps and communities in western Tanzania where tTEM surveys were conducted for this paper. In this part of the country electrification was often limited to a few powerlines branching from the main lines along the highway to service a few buildings within a community of thousands. Here, powerlines concerns, which effectively prevent or severely restrict TEM coverage in heavily-populated areas in developed nations were not a significant problem. However, buildings or other infrastructure (e.g., metal fences) can also potentially interfere with TEM data, corrupting it to a point where reliable data inversion and subsequent

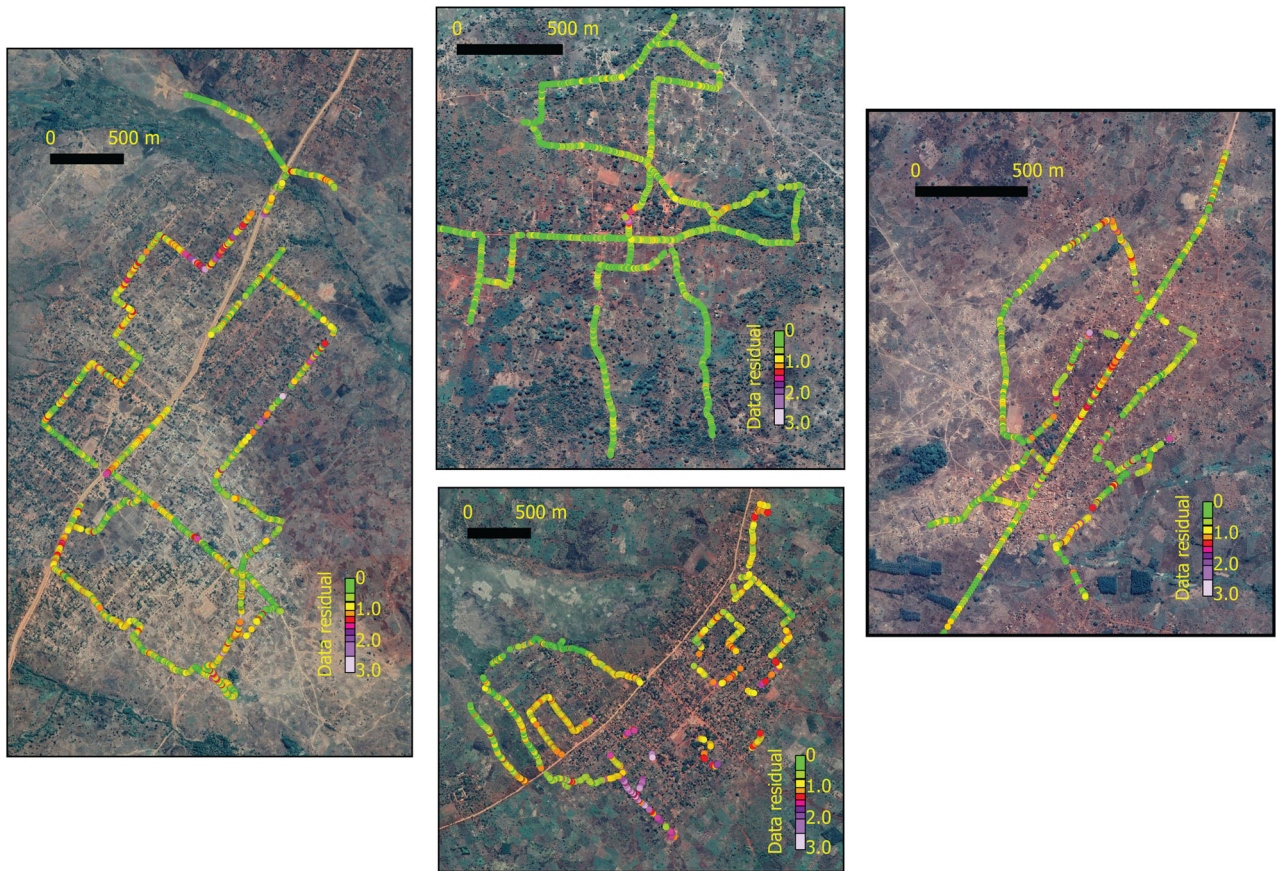


Figure 11. Satellite images of four host communities with tTEM data residuals superimposed. Map data: Google, Maxar Technologies, CNES/Airbus.

geological interpretations cannot be made. One concern was whether metal sheeting or that commonly serves as roofs or walls for many structures would lead to coupling strong enough to disturb TEM data.

In Figure 11, profiles of tTEM model data-fit are superimposed on satellite imagery for four communities in western Tanzania. These communities were selected as part of a well-installation program to-be carried out by Water Mission Tanzania, where these surveys function as a predrilling regional investigation to locate attractive borehole sites. During these surveys, rough terrain (brushy or forested) generally restricted tTEM access to existing roads and footpaths. Roads were deemed satisfactory for data collection as they are dirt roads lacking any buried cables. Each of the four surveys required a single day of data collection, where approximately 17, 12, 14, and 12km of data were produced in each case. The colored dots indicate regions where data was collected and subsequently inverted to produce a 1D resistivity model of the local underlying electrical resistivity. The color of the dot illustrates the quality of the data fit, where data fits corresponding a χ^2 value of approximately 1 are considered to have satisfactorily fit the data within the uncertainty, and the corresponding models are therefore considered trustworthy. In some locations, data gaps are present due to the proximity to a powerline or turning of the system (this requires culling of data because the

system is not in a straight line). However, χ^2 value of approximately 1 can also be produced in the presence of galvanic couplings, a phenomenon occurring when currents are induced in nearby conductors, such as buried cables. In these cases, the resulting models are not representative of the subsurface despite a good data fit. These situations can be identified as they are often spatially isolated (i.e., in close vicinity of the conductor, and often appear as linear features following the buried cable). These anomalies must be identified and culled from the final set of models.

As seen in Figure 11, many of the lines traverse through the town, often passing within several meters of buildings (many with metal sheeting for walls or roofs). The images indicate that almost all surveys have satisfactory data fits and high-quality data were obtained within the communities themselves. It is unlikely that galvanic couplings have strongly influenced the data given the consistent observation of lateral continuity in the resistivity images as one traverses from the exterior to the interior of the community. The ability to survey within nonelectrified communities near existing structures may allow for dense 3D hydrogeological interpretations in close vicinity to the communities. This is an important observation, as it can at times be advantageous to locate sustainable water sources close to where people using the water live, because infrastructure costs and the

daily burden of water collection increase as the distance between the water source and point of use increases. The ability to collect high-quality data in close proximity to the communities using tTEM makes this a possibility.

Discussion

During the field campaign in Tanzania, typical daily tTEM production rates ranged from about 10 km/day to as much as 25 km/day, with the production rate mostly dependent on terrain and vehicle accessibility. As such, a relatively small field team (consisting of 2 to 3 people) is capable of mapping relatively large regions in a short amount of time. A single day of tTEM surveying is often sufficient to provide comprehensive coverage of the area surrounding a small to moderately sized community. The tTEM method provides several orders-of-magnitude increase in production rate and data density compared to the spatial coverage possible from alternative (nonairborne) geophysical methods (e.g., conventional TEM, VES, or ERT).

Reliable interpretation of the tTEM results and successful application of the method requires some knowledge of the regional and/or local hydrogeological setting. Developing an understanding of the electrical resistivity to hydrogeological unit or property transform is critical to ensuring robust conceptual models are developed. Knowledge of the common hydrogeologic characteristics in locally successful wells is extremely valuable information, as the characteristics of successful wells can help identify targets that can be located in the tTEM images and guide decisions toward sites with a greater probability of drilling success. Pairing a hydrogeologist with local knowledge with tTEM mapping capabilities offers great potential to rapidly produce a high-quality conceptual models in regions with limited supporting data.

From a financial perspective, application of the tTEM method can be considered a risk-mitigation tool. For a cost often much less than that of a single well, a regional or multicomunity exploration survey can be undertaken to deliver critical information required to inform decision-makers about potential well locations. The alternative, well-siting in the absence of supporting data or in the presence of large uncertainties exposes one to a higher risk of failure. For projects or campaigns intended to drill multiple wells, the small expense of geophysical exploration capable of increasing the probability of drilling a successful well shows great potential to translate into a fixed budget reaching a larger number of people or siting higher yielding wells. Ultimately, the goal is to improve drilling success rates from the unacceptably low percentages in many data-poor regions (Wright 1992). It is worth noting that for larger drilling campaigns, the interpretation scheme for the tTEM results should be updated regularly to reflect the information from each drilled well, where comparison of lithology logs collected during drilling can provide valuable input to better constrain the local electrical resistivity to hydrogeology

transform, and where possible should include borehole geophysical logging (e.g., EM induction, electric, natural gamma logs, etc.) to aid the development of the resistivity-hydrogeologic property transform.

Limitations of the tTEM method include the requirement to operate over terrain that is passable using an all-terrain vehicle (ATV), and that the depth of investigation is limited to approximately 80 to 100 m. In many cases, brushy or forested terrain cannot be navigated using the tTEM system without requiring manual movement of the system around obstacles (because the 11 m-long system cannot make right-angle turns). Large boulders or rocky-terrain common at outcrops also limits system access, although in certain cases the system can still pass difficult terrain at slow driving speeds. In cases where deeper aquifer systems are the target (>100 m depth), although tTEM cannot necessarily resolve targets at these great depths, the results can still provide valuable insights into local subsurface conditions—such as the protection of these deep units from potential contamination at the surface—or if they are isolated from shallower groundwater systems. The challenge stems from attempting to image a resistive target (weathered bedrock layer in this case) beneath a conductive unit (saprolite). In regions with thicker saprolite layers it was difficult to penetrate beneath this layer, as the conductive layer attenuates the electromagnetic fields.

In future campaigns, the use of geophysical logs in combination with tTEM surveys could greatly enhance hydrological interpretations. Resistivity and gamma logs could help provide valuable high-resolution measures at depth that could be used to calibrate local geophysics to geology transforms, which ultimately can help enhance the accuracy of the resulting conceptual understanding of the local hydrological system.

Conclusion

When little to no supplementary information about local hydrological units is available, well-siting is often plagued by large uncertainties that may culminate in poor success-rates for wells. In these situations, the tTEM method can provide a rapid, cost-efficient means to map local-to-regional hydrogeology, and to enhance what little hydrogeological data is available. The resulting high-resolution 3D images of local hydrogeological units provide valuable insights for well-siting including mapping of the lateral continuity/extent, depths, and thicknesses of potential aquifers/aquitards. In this work, the tTEM system provided robust results under challenging field conditions, including the acquisition of usable data within communities with low-density electrification and near buildings with metal roofs and walls. Interpretation of the tTEM resistivity profiles resulted in the successful siting of a high-yielding well in a community named Makere, as well as attractive locations for future boreholes in four other communities and two refugee camps. Furthermore, the tTEM system is well-suited to mapping in regolith settings, where lateral continuity

and thickness of the upper laterite and saprolite units can be well-imaged. Overall, the tTEM system shows great promise for use in developing countries to increase the likelihood of drilling successful wells in the settings where little supporting hydrogeologic data is available.

Acknowledgments

This work was supported by funding from the Poul Due Jensen Foundation—under the SiTEM project. The authors would also like to thank Water Mission Tanzania for their significant efforts in helping to execute and coordinate logistics for the field campaign in Tanzania.

Authors' Note

The authors do not have any conflicts of interest or financial disclosures to report.

References

- Alle, I.C., M. Descloitres, J.M. Vouillamoz, N. Yalo, F.M.A. Lawson, and A.C. Adihou. 2018. Why 1D electrical resistivity techniques can result in inaccurate siting of boreholes in hard rock aquifers and why electrical resistivity tomography must be preferred: The example of Benin, West Africa. *Journal of African Earth Sciences* 139: 341–353.
- Auken, E., N. Foged, J.J. Larsen, K.V.T. Lassen, P.K. Maurya, S.M. Dath, and T.T. Eiskjær. 2019. tTEM—A towed transient electromagnetic system for detailed 3D imaging of the top 70 m of the subsurface. *Geophysics* 84, no. 1: E13–E22.
- Auken, E., T. Boesen, and A.V. Christiansen. 2017. A review of airborne electromagnetic methods with focus on geotechnical and hydrological applications from 2007 to 2017. *Advances in Geophysics* 58: 47–93.
- Auken, E., A.V. Christiansen, B.H. Jacobsen, N. Foged, and K.I. Sørensen. 2005. Piecewise 1D laterally constrained inversion of resistivity data. *Geophysical Prospecting* 53, no. 4: 497–506.
- Beauvais, A., M. Ritz, J.C. Parisot, M. Dukhan, and C. Bantsimba. 1999. Analysis of poorly stratified lateritic terrains overlying a granitic bedrock in West Africa, using 2-D electrical resistivity tomography. *Earth and Planetary Science Letters* 173, no. 4: 413–424.
- Butt, C.R., M.J. Lintern, and R.R. Anand. 2000. Evolution of regoliths and landscapes in deeply weathered terrain—Implications for geochemical exploration. *Ore Geology Reviews* 16, no. 3–4: 167–183.
- Butt, C.R.M., and H. Zeegers. 1992. Climate, geomorphological environment and geochemical dispersion models. *Regolith Exploration Geochemistry in Tropical and Subtropical Terrains* 4: 3–24.
- Butt, C.R.M., D.J. Gray, M.J. Lintern, I.D.M. Robertson, G.F. Taylor, and K.M. Scott. 1991. Gold and associated elements in the regolith-dispersion processes and implications for exploration. CSIRO/AMIRA Weathering Processes Project P241. Final report.
- Chongo, M., A.V. Christiansen, A. Tembo, K.E. Banda, I.A. Nyambe, F. Larsen, and P. Bauer-Gottwein. 2015. Airborne and ground-based transient electromagnetic mapping of groundwater salinity in the Machile-Zambezi Basin, southwestern Zambia. *Near Surface Geophysics* 13, no. 4: 383–396.
- Choudhury, J., K.L. Kumar, E. Nagaiah, S. Sonkamble, S. Ahmed, and V. Kumar. 2017. Vertical electrical sounding to delineate the potential aquifer zones for drinking water in Niamey city, Niger, Africa. *Journal of Earth System Science* 126, no. 6: 91.
- Christiansen, A.V., and E. Auken. 2012. A global measure for depth of investigation. *Geophysics* 77, no. 4: WB171–WB177.
- Christiansen, A.V., E. Auken, and K.I. Sørensen. 2006. The transient electromagnetic method. In *Groundwater Geophysics*, 179–225. Berlin, Heidelberg: Springer.
- Coker, J.O. 2012. Vertical electrical sounding (VES) methods to delineate potential groundwater aquifers in Akobo area, Ibadan, South-western, Nigeria. *Journal of Geology and Mining Research* 4, no. 2: 35–42.
- Fitterman, D.V., and V.F. Labson. 2005. Electromagnetic induction methods for environmental problems. In *Near-Surface Geophysics*, 301–356. Tulsa: Society of Exploration Geophysicists.
- Fountain, D. 1998. Airborne electromagnetic systems-50 years of development. *Exploration Geophysics* 29, no. 2: 1–11.
- Harvey, P. 2004. Borehole sustainability in rural Africa: An analysis of routine field data. In *Proceedings of the 2004 WEDC International Conference*, 147–150. Leicestershire, UK: Water, Eng. and Dev. Cent. Loughborough University.
- Klee, P. 2013. Greater water security with groundwater—Groundwater mapping and sustainable groundwater management. The Rethink Water network and Danish Water Forum white papers, Copenhagen. <https://um.dk/da/~media/Irland/Documents/White%20paper%20-%20Groundwater%20mapping%20FINAL%20March%202013.pdf> (accessed March 2013).
- Magaia, L.A., T.N. Goto, A.A. Masoud, and K. Koike. 2018. Identifying groundwater potential in crystalline basement rocks using remote sensing and electromagnetic sounding techniques in central western Mozambique. *Natural Resources Research* 27, no. 3: 275–298.
- Minsley, B.J. 2011. A trans-dimensional Bayesian Markov chain Monte Carlo algorithm for model assessment using frequency-domain electromagnetic data. *Geophysical Journal International* 187, no. 1: 252–272.
- Palacky, G.J. 1988. Resistivity characteristics of geologic targets. *Electromagnetic Methods in Applied Geophysics* 1: 53–129.
- Peric, M. 1981. Exploration of Burundi nickeliferous laterites by electrical methods. *Geophysical Prospecting* 29, no. 2: 274–287.
- Sakala, E., A. Tessema, and P.K. Nyabeze. 2014. Regional interpretation of aeromagnetic data for groundwater exploration in Capricorn District, Limpopo, South Africa. *International Journal of Modelling and Simulation* 34, no. 1: 36–42.
- Safe Drinking Water Foundation (2017). Groundwater. <https://www.safewater.org/fact-sheets-1/2017/1/23/groundwater> (accessed March 31, 2020).
- Street, G., A. Duncan, P. Fullagar, and R. Tresidder. 2018. Loupe—a portable EM profiling system. *Australian Society of Exploration Geophysicists Extended Abstracts* 1: 1–3. https://doi.org/10.1071/ASEG2018abW10_3G
- Van Overmeeren, R.A. 1981. A combination of electrical resistivity, seismic refraction, and gravity measurements for groundwater exploration in Sudan. *Geophysics* 46, no. 9: 1304–1313.
- Viezzoli, A., A.V. Christiansen, E. Auken, and K.I. Sørensen. 2008. Quasi-3D modeling of airborne TEM data by spatially constrained inversion. *Geophysics* 73, no. 3: F105–F113.
- Vignoli, G., G. Fiandaca, A.V. Christiansen, C. Kirkegaard, and E. Auken. 2015. Sharp spatially constrained inversion with applications to transient electromagnetic data. *Geophysical Prospecting* 63, no. 1: 243–255.

- Vouillamoz, J.M., F.M.A. Lawson, N. Yalo, and M. Descloitres. 2014. The use of magnetic resonance sounding for quantifying specific yield and transmissivity in hard rock aquifers: The example of Benin. *Journal of Applied Geophysics* 107: 16–24.
- World Health Organization (WHO). 2019. Fact sheets—Detail—Drinking water. <https://www.who.int/news-room/fact-sheets/detail/drinking-water> (accessed March 31, 2020).
- WHO/UNICEF Joint Water Supply, Sanitation Monitoring Programme, World Health Organization, & UNICEF. 2008. *Progress on Drinking Water and Sanitation: Special Focus on Sanitation*. New York: World Health Organization.
- Wright, E.P. 1992. The hydrogeology of crystalline basement aquifers in Africa. *Geological Society, London, Special Publications* 66, no. 1: 1–27.
- Yang, D., and D.W. Oldenburg. 2012. Three-dimensional inversion of airborne time-domain electromagnetic data with applications to a porphyry deposit. *Geophysics* 77, no. 2: B23–B34.